

Chemical analysis of CH stars – II. Atmospheric parameters and elemental abundances

Drisya Karinkuzhi^{1,2★} and Aruna Goswami¹

¹*Indian Institute of Astrophysics, Koramangala, Bangalore 560034, India*

²*Department of physics, Bangalore university, Jnana Bharathi Campus, Karnataka 560056, India*

Accepted 2014 October 3. Received 2014 October 2; in original form 2014 April 16

ABSTRACT

We present detailed chemical analyses for a sample of 12 stars selected from the CH star catalogue of Bartkevicius. The sample includes two confirmed binaries, four objects that are known to show radial velocity variations and the rest with no information on the binary status. A primary objective is to examine if all these objects exhibit chemical abundances characteristics of CH stars, based on detailed chemical composition study using high-resolution spectra. We have used high-resolution ($R \sim 42\,000$) spectra from the ELODIE archive. These spectra cover 3900 to 6800 Å in the wavelength range. We have estimated the stellar atmospheric parameters, the effective temperature T_{eff} , the surface gravity $\log g$, and metallicity $[\text{Fe}/\text{H}]$ from local thermodynamic equilibrium analysis using model atmospheres. Estimated temperatures of these objects cover a wide range from 4200 to 6640 K, the surface gravity from 0.6 to 4.3 and metallicity from -0.13 to -1.5 . We report updates on elemental abundances for several heavy elements, Sr, Y, Zr, Ba, La, Ce, Pr, Nd, Sm, Eu and Dy. For the object HD 89668, we present the first abundance analyses results. Enhancement of heavy elements relative to Fe, a characteristic property of CH stars is evident from our analyses in the case of four objects, HD 92545, HD 104979, HD 107574 and HD 204613. A parametric-model-based study is performed to understand the relative contributions from the s- and r-process to the abundances of the heavy elements.

Key words: stars: abundances – stars: carbon – stars: late-type – stars: Population II.

1 INTRODUCTION

CH stars are characterized by iron deficiency and enhancement of carbon and s-process elements. Majority of the CH stars are known as binaries with white dwarf companions that are presently not visible (McClure 1983, 1984, McClure & Woodsworth 1990). The companion white dwarfs produced heavy elements while passing through the asymptotic giant branch (AGB) stage of evolution; these material are received by the CH stars through mass transfer enriching their surface chemical composition. CH stars thus provide an important means to study the production and distribution of heavy elements arising from AGB nucleosynthesis.

In spite of their usefulness, literature survey reveals that detailed chemical composition studies are not available for many CH stars. The CH star catalogue of Bartkevicius (1996) lists about 261 objects, 17 of which belong to ω Cen globular cluster. Many of the objects listed in this catalogue have no information on binary status.

It would be interesting to compare and examine the abundance patterns of elements observed in the confirmed binaries with their counterparts in objects that have no information on binary status. While long-term radial velocity monitoring are expected to throw light on the binary status, detailed chemical composition studies could also reflect on the binary origin.

Previous studies along this line include a detailed chemical composition study of 10 objects from the Bartkevicius catalogue by Karinkuzhi & Goswami (2014, hereafter Paper I). This study revealed that only five objects out of 10, exhibit abundances of heavy elements with $[\text{Ba}/\text{Fe}] > 1$, a characteristic of CH stars. Four objects show either near-solar values or $[\text{Ba}/\text{Fe}] < 0$. The remaining one object, HD 4395 gave $[\text{Ba}/\text{Fe}] \sim 0.79$. Based on their analyses, the authors concluded that out of 10, only five objects are bonafide CH stars.

As far as the chemical composition is concerned, CH stars (with $-0.2 < [\text{Fe}/\text{H}] < -2$) and the class of carbon-enhanced metal-poor (CEMP)-s ($[\text{C}/\text{Fe}] > 1$, $[\text{Fe}/\text{H}] < -2$; Beers & Christlieb 2005) stars are believed to have a similar origin. Medium-resolution spectral analyses of about 300 faint high latitude carbon stars of Hamburg/ESO survey (Christlieb et al. 2001) have shown that about

★ E-mail: drisya@iiap.res.in

33 per cent of the objects are potential CH star candidates (Goswami 2005; Goswami et al. 2007; Goswami, Karinkuzhi & Shantikumar 2010a). Analyses of high-resolution Subaru spectra for a sample of them, have shown the object HE 1152–0355 to be a CH star, and HE 1305+0007, a CEMP-r/s star (Goswami et al. 2006). A large fraction of CEMP-s and CEMP-r/s stars show radial velocity variations, based on which these stars are suggested to be all binaries (Lucatello et al. 2005), and that the CEMP-s stars are the more metal-poor counterparts of CH stars.

Although high-resolution spectroscopic analyses of CEMP stars have shown that a variety of production mechanisms are needed to explain the observed range of elemental abundance patterns in them, it is widely accepted that the binary scenario of CH star formation is the most likely formation mechanism also for CEMP-s stars (Norris, Ryan & Beers 1997a,b; Aoki et al. 2001, 2002a, 2002b, 2007; Norris et al. 2002; Barbuy et al. 2005; Lucatello et al. 2005; Goswami et al. 2006; Goswami & Aoki 2010).

In this work, we have considered another 12 objects from the catalogue of Bartkevicius (1996) for a detailed chemical composition study. Detailed high-resolution spectroscopic analyses for this sample of objects are either not available in the literature or limited by resolution or wavelength range. Polarimetric studies of carbon stars by Goswami & Karinkuzhi (2013) include six objects from this sample. Among these, three objects show percentage *V*-band polarization at a level ~ 0.2 per cent (HD 55496 (p_v per cent ~ 0.18), HD 111721 (p_v per cent ~ 0.22), and HD 164922 (p_v per cent ~ 0.28)) indicating presence of circumstellar dust distribution in non-spherically symmetric envelopes. The other three objects, HD 92545, HD 107574 and HD 126681, show *V*-band percentage polarization at a level < 0.1 per cent.

The sample of programme stars includes two confirmed binaries, HD 122202 and HD 204613. Four objects in this sample, HD 55496, HD 92545, HD 104979 and HD 107574 are known to show radial velocity variability, and for the rest, none of these two information is available. In the following text, for convenience, we will refer the objects that are confirmed binaries as group 1 objects, those with limited radial velocity information as group 2 objects and the objects for which none of these information are available as group 3 objects. One of our primary objectives is to estimate the abundances of heavy elements and critically examine the abundance patterns and abundance ratios to check if they exhibit characteristic abundance patterns of CH stars.

Among CEMP stars, the group of CEMP-r/s stars show enhancement of both r- and s-process elements ($0 < [\text{Ba}/\text{Eu}] < 0.5$; Beers & Christlieb 2005). None of our objects in the sample are found to show $[\text{Ba}/\text{Eu}]$ ratios in this range. Four objects show characteristic heavy element abundance patterns of CH stars. Based on our analyses, the others certainly do not belong to this class of objects.

Source of the high-resolution spectra is described in Section 2. Estimates of radial velocities are presented in Section 3. Temperature estimates from photometry are discussed in Section 4. Estimation of stellar atmospheric parameters are presented in Section 5. Results of abundance analysis are discussed in Section 6. In Section 7, we present brief discussions on each individual star. Estimated stellar masses are discussed in Section 8. A discussion on the parametric model based analysis is presented in Section 9. Conclusions are drawn in Section 10.

2 SPECTRA OF THE PROGRAMME STARS

Low-resolution spectra of these objects obtained from 2m Himalayan Chandra Telescope at the Indian Astronomical Ob-

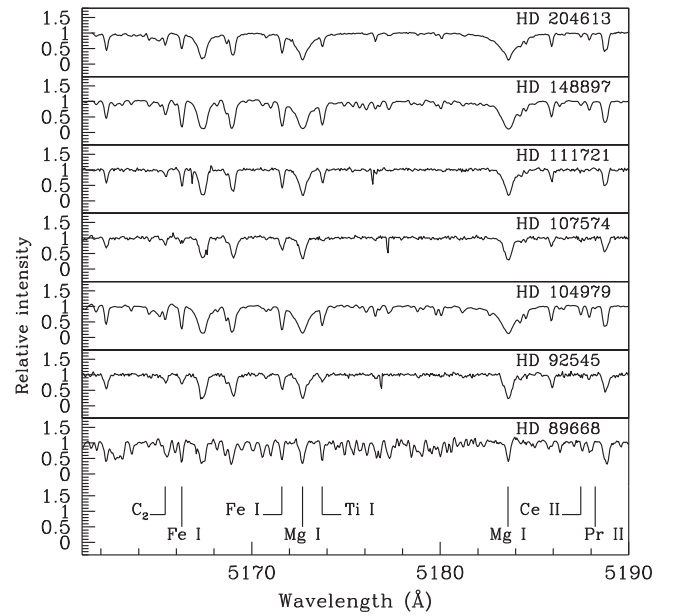


Figure 1. Sample spectra of a few programme stars in the wavelength region 5160 to 5190 Å.

servatory, Hanle using HFOSC clearly show strong features due to carbon. HFOSC is an optical imager cum spectrograph for conducting low- and medium-resolution grism spectroscopy (<http://www.iiap.res.in/fao/hfosc.html>). High-resolution spectra necessary for abundance analyses of the programme stars are taken from the ELODIE archive (Moultaka et al. 2004). This archive contains a large collection of high-resolution spectra acquired with the 1.93 m telescope at the Observatoire de Haute Provence using the ELODIE spectrograph (Baranne et al. 1996). An online reduction software program TACOS automatically performs optimal extraction and wavelength calibration of data. The spectra consist of 67 orders with near-constant interorder spacing. The resolution of the spectra is $\sim 42\,000$ and cover the wavelength range 3900 to 6800 Å. A few sample spectra are shown in Figs 1 and 2. The basic data for the programme stars obtained from the SIMBAD data base are listed in Table 1.

3 RADIAL VELOCITY

Radial velocities of the programme stars are calculated using a selected set of clean unblended lines in the spectra. Estimated mean radial velocities along with the standard deviation of the mean values are presented in Table 2. The literature values are also presented for a comparison. Reports on radial velocity variations for a large number of CH and barium stars are available in literature (McClure 1984, 1997; McClure & Woodworth 1990). McClure (1997) has reported the radial velocity variations and orbital parameters for two sub-giant CH stars HD 122202 and HD 204613. These objects are confirmed binaries. Although radial velocity variations are noticed in HD 55496, it is not confirmed as binary. Our estimate also shows a difference of 7 km s^{-1} from the literature value. Mild radial velocity variations are also noticed in HD 92545 and HD 107574 (North & Duquennoy 1992). Our radial velocity estimates of HD 104979 and HD 164922 show a difference of $\sim 15\text{ km s}^{-1}$ from the literature values.

Table 1. Basic data for the programme stars.

Star name.	RA(2000)	Dec.(2000)	<i>B</i>	<i>V</i>	<i>J</i>	<i>H</i>	<i>K</i>
HD 55496	07 12 11.37	−22 59 00.61	9.30	8.40	6.590	6.043	5.931
HD 89668	10 20 43.40	−01 28 11.38	10.50	9.41	7.443	6.908	6.760
HD 92545	10 40 57.70	−12 11 44.23	9.07	8.56	7.548	7.347	7.282
HD 104979	12 05 12.54	+08 43 58.74	5.10	4.13	2.459	1.987	1.869
HD 107574	12 21 51.86	−18 24 00.15	8.99	8.54	7.660	7.460	7.415
HD 111721	12 51 25.19	−13 29 28.17	8.78	7.97	6.347	5.898	5.786
HD 122202	14 00 18.96	+04 51 25.06	9.85	9.36	8.506	8.358	8.252
HD 126681	14 27 24.91	−18 24 40.43	9.93	9.32	8.044	7.709	7.631
HD 148897	16 30 33.54	+20 28 45.07	6.50	5.25	2.950	2.248	1.966
HD 164922	18 02 30.86	+26 18 46.80	7.79	6.99	5.553	5.203	5.113
HD 167768	18 16 53.10	−03 00 26.64	6.89	6.00	4.376	3.906	3.789
HD 204613	21 27 42.96	+57 19 18.86	8.86	8.22	7.100	6.824	6.788

Table 2. Radial velocities.

Star name	V_r km s ^{−1} (our estimates)	V_r km s ^{−1} (from literature)	Reference
HD 55496	315.28 ± 0.80	322.00	1
HD 89668	22.84 ± 0.70	23.0	2
HD 92545	−17.51 ± 0.65	−16.65	3
HD 104979	−45.40 ± 0.42	−29.62	4
HD 107574	−16.33 ± 0.72	−29.40	1
HD 111721	20.59 ± 0.67	21.40	1
HD 122202	−7.40 ± 0.97	−10.5	6
HD 126681	−45.36 ± 0.46	−45.58	7
HD 148897	17.55 ± 0.71	18.40	1
HD 164922	34.86 ± 0.91	20.29	8
HD 167768	1.39 ± 0.42	1.60	1
HD 204613	−89.53 ± 0.33	−90.96	5

Notes: 1. Gontcharov (2006), 2. Soubiran et al. (2008), 3. Siebert et al. (2011), 4. Massarotti et al. (2008), 5. Pourbaix et al. (2004), 6. Luck & Bond (1991), 7. Santos et al. (2011), 8. Nidever et al. (2002).

4 TEMPERATURES FROM PHOTOMETRIC DATA

Temperatures from photometric data are estimated following the procedure discussed in Paper I. Here, we mention a few points relevant to this work. Colour–temperature calibrations of Alonso, Arribas & Martinez-Roger (1996) are used for photometric temperature determination. These calibrations were derived by using a large number of lower main-sequence stars and sub-giants, whose temperatures were measured by the infrared flux method, and hold within temperature and metallicity ranges of $4000 \text{ K} \leq T_{\text{eff}} \leq 7000 \text{ K}$ and metallicity between -2.5 and 0.0 . The uncertainty in the temperature calibrations is $\sim 100 \text{ K}$. Although the difference between 2MASS infrared photometric system and photometry data measured on the TCS (Telescopio Carlos Sanchez) system used by Alonso et al. (1996, 1999), to derive the T_{eff} scales is very small, we have used the necessary transformations between the different photometric systems from Ramirez & Melendez (2004) and Alonso et al. (1996) and Alonso, Arribas & Martinez-Roger (1999). The equations are

$$J_{\text{TCS}} = J_{2\text{MASS}} + 0.001 - 0.049(J_{2\text{MASS}} - K_{2\text{MASS}})$$

$$H_{\text{TCS}} = H_{2\text{MASS}} - 0.018 + 0.003(J_{2\text{MASS}} - K_{2\text{MASS}})$$

$$K_{\text{TCS}} = K_{2\text{MASS}} - 0.014 + 0.034(J_{2\text{MASS}} - K_{2\text{MASS}})$$

$$K_J = K_{\text{TCS}} + 0.042 - 0.019((J_{\text{TCS}} - K_{\text{TCS}}) - 0.008)/0.910)$$

$$(V - K)_{\text{TCS}} = 0.050 + 0.993(V - K_J)$$

$$\theta_{JK} = 0.582 + 0.799(J_{\text{TCS}} - K_{\text{TCS}}) + 0.085(J_{\text{TCS}} - K_{\text{TCS}})(J_{\text{TCS}} - K_{\text{TCS}})$$

$$\theta_{JH} = 0.587 + 0.922(J_{\text{TCS}} - H_{\text{TCS}}) + 0.218(J_{\text{TCS}} - H_{\text{TCS}})(J_{\text{TCS}} - H_{\text{TCS}}) + 0.016(M)(J_{\text{TCS}} - H_{\text{TCS}})$$

$$\theta_{VK} = 0.555 + 0.195(V - K)_{\text{TCS}} + 0.013(V - K)_{\text{TCS}}(V - K)_{\text{TCS}} - 0.008(V - K)_{\text{TCS}}(M) + 0.009(M) - 0.002M^2$$

$$T_{\text{eff}(xy)} = 5040/\theta_{(xy)},$$

where M is the metallicity of the star, xy indicates the JK , JH and VK . For two objects, temperatures derived from both spectroscopic method and photometric method are similar. Among the rest for most of the objects, the derived T_{eff} from $V - K$ is $\sim 350 \text{ K}$, and from $J - H$ is $\sim 300 \text{ K}$ less than the adopted spectroscopic T_{eff} . The temperature calibrations from the $T_{\text{eff}} - (J - H)$ and $T_{\text{eff}} - (V - K)$ relations involve a metallicity ($[\text{Fe}/\text{H}]$) term. Estimates of T_{eff} at four assumed metallicity values (shown in parenthesis) are listed in Table 3.

5 STELLAR ATMOSPHERIC PARAMETERS

The set of Fe I and Fe II lines used for the present analysis to find the stellar atmospheric parameters are listed in Tables 4A and 4B. The excitation potential of the lines are in the range 0.0 – 5.0 eV and equivalent width in the range 20 – 180 \AA . We have assumed local thermodynamic equilibrium (LTE) for our calculations. A recent version of MOOG of Sneden (1973) is used. Model atmospheres (available at <http://cfaku5.cfa.harvard.edu/> and labelled with a suffix *odfnew*) were selected from the Kurucz grid of model atmospheres with no convective overshooting. Solar abundances are taken from Asplund, Grevesse & Sauval (2005).

The microturbulent velocity is estimated at a given effective temperature by demanding that there be no dependence of the derived Fe I abundance on the equivalent width of the corresponding lines.

The effective temperature is determined by making the slope of the abundance versus excitation potential of Fe I lines to be nearly zero. The initial value of temperature is taken from the photometric estimates and arrived at a final value by an iterative method with the slope nearly equal to zero. Figs 3 and 4 show abundance of Fe I and Fe II as a function of excitation potential and equivalent widths respectively.

Table 3. Temperatures from photometry.

Star name	T_{eff} ($J-K$)	$T_{\text{eff}}(-0.5)$ ($J-H$)	$T_{\text{eff}}(-0.5)$ ($V-K$)	$T_{\text{eff}}(-1.0)$ ($J-H$)	$T_{\text{eff}}(-1.0)$ ($V-K$)	$T_{\text{eff}}(-1.5)$ ($J-H$)	$T_{\text{eff}}(-1.5)$ ($V-K$)	$T_{\text{eff}}(-0.5)$ ($B-V$)	$T_{\text{eff}}(-1.0)$ ($B-V$)	$T_{\text{eff}}(-1.5)$ ($B-V$)	Spectroscopic estimates
HD 55496	4542.90	4441.94	4502.61	4458.65	4487.14	4475.49	4475.76	4774.22	4668.96	4591.12	4850
HD 89668	4462.68	4502.02	4518.76	4535.63	4318.91	4302.05	4288.96	4339.62	4246.01	4175.29	5400
HD 92545	6343.00	6422.81	6088.75	6436.34	6095.01	6449.92	6108.68	6159.33	6014.42	5914.10	6380
HD 104979	5025.77	5056.49	4896.90	5073.13	4885.21	5089.87	4878.30	4604.59	4503.92	4428.86	5060
HD 107574	6605.48	6892.23	6774.10	6903.73	6795.30	6915.27	6825.87	6847.21	6681.19	6569.80	6250
HD 111721	–	4601.48	6451.12	4618.25	6464.85	4635.14	6486.97	5011.10	4899.33	4817.63	5212
HD 122202	6417.84	6878.47	6890.04	6901.64	6370.16	6382.14	6402.28	6329.12	6179.09	6076.03	6430
HD 126681	5539.93	5508.00	5524.06	5540.22	5452.94	5448.38	5449.71	5629.53	5500.24	5408.49	5760
HD 148897	3635.13	3885.78	3762.86	3901.90	3743.08	3918.15	3726.27	4015.00	3929.84	3864.45	4285
HD 164922	5412.07	5422.44	5191.94	5438.65	5183.77	5454.94	5180.94	5038.84	4926.30	4844.15	5400
HD 167768	4841.08	4060.94	4910.98	4077.32	4899.44	4093.83	4892.70	4799.45	4693.50	4615.26	5070
HD 204613	6070.18	5869.04	5841.82	5884.32	5843.53	5899.68	5852.03	5494.19	5368.80	5279.24	5875

Note: The numbers in the parenthesis indicate the metallicity values at which the temperatures are calculated. Temperatures are given in Kelvin.

Table 4A. Fe lines used for deriving atmospheric parameters for the first six objects.

Wavelength (Å)	Element	E_{low} (eV)	$\log gf$	HD 55496	HD 89668	HD 92545	HD 104979	HD 107574	HD 111721
4062.440	Fe I	2.850	−0.860	–	–	110.3	–	–	–
4114.440		2.830	−1.300	–	–	–	–	–	–
4132.900		2.850	−1.010	–	–	–	–	–	–
4143.870		1.560	−0.510	–	–	–	–	–	–
4147.670		1.490	−2.100	–	–	–	–	–	–
4153.900		3.400	−0.320	–	–	–	–	–	–
4154.500		2.830	−0.690	–	–	–	–	–	–
4184.890		2.830	−0.870	–	–	151.2	143.1	–	–

Note: This table is available in its entirety in online only. A portion is shown here for guidance regarding its form and content.

Table 4B. Fe lines used for deriving atmospheric parameters for the next six objects.

Wavelength (Å)	Element	E_{low} (eV)	$\log gf$	HD 122202	HD 126681	HD 148897	HD 164922	HD 167768	HD 204613
4062.440	Fe I	2.850	−0.860	–	–	–	–	–	−102.9
4114.440		2.830	−1.300	–	–	129.8	–	–	–
4132.900		2.850	−1.010	–	–	–	–	–	107.6
4143.870		1.560	−0.51	–	–	–	–	–	–
4147.670		1.490	−2.100	–	–	–	–	–	114.6
4153.900		3.400	−0.320	–	–	–	–	–	–
4154.500		2.830	−0.690	–	–	–	–	–	–
4184.890		2.830	−0.870	–	–	–	–	–	105.0

Note: This table is available in its entirety in online only. A portion is shown here for guidance regarding its form and content.

The surface gravity is fixed at a value that gives same abundances for Fe I and Fe II lines. Derived atmospheric parameters are listed in Table 5.

6 ABUNDANCE ANALYSIS

Elemental abundances are calculated from the measured equivalent widths of lines due to neutral and ionized elements using a recent version of MOOG of Sneden (1973) and the adopted model atmospheres. A master line list of all the elements is generated comparing the spectra of the programme stars with the spectrum of Arcturus. The presented line lists contain only those lines which are used for abundance calculation. Even though we could detect many lines for each element, only a few were usable for abundance calculation, the others being either distorted or blended with contributions from other species. The $\log gf$ values of the atomic lines are taken from literature consulting various sources, such as, Aoki et al. (2005, 2007), Goswami et al. (2006), Jonsell et al. (2006),

Table 5. Derived atmospheric parameters and carbon isotopic ratios for the programme stars.

Star name	T_{eff} K	$\log g$	ζ km s ^{−1}	[Fe I/H]	[Fe II/H]	C^{12}/C^{13}
HD 55496	4850	2.05	1.52	−1.49	−1.41	4
HD 89668	5400	4.35	2.35	−0.13	−0.19	19.1
HD 92545	6380	4.65	1.45	−0.21	−0.22	–
HD 104979	5060	2.67	1.55	−0.26	−0.31	9.9
HD 107574	6250	2.9	1.35	−0.65	−0.60	–
HD 111721	5212	2.6	1.30	−1.11	−1.11	–
HD 122202	6430	4.0	2.08	−0.63	−0.65	13.2
HD 126681	5760	4.65	0.9	−0.90	−0.92	–
HD 148897	4285	0.6	1.83	−1.02	−0.99	13
HD 164922	5400	4.3	0.09	0.22	0.23	12
HD 167768	5070	2.55	1.49	−0.51	−0.56	–
HD 204613	5875	4.2	1.22	−0.24	−0.24	11.1

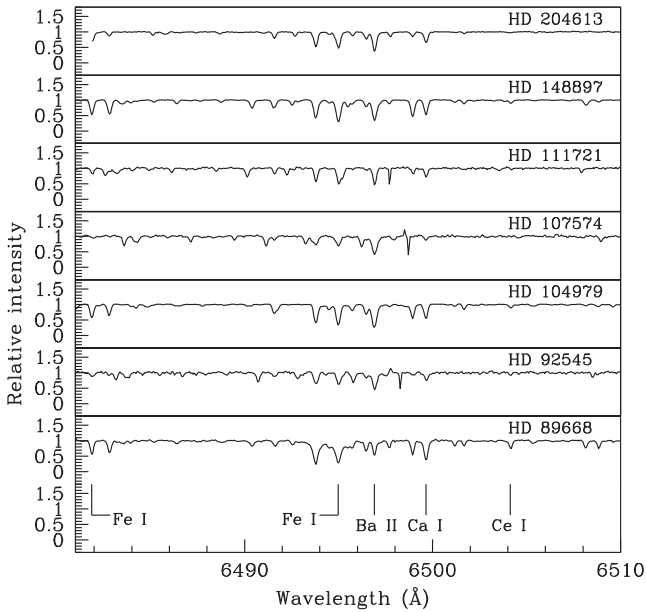


Figure 2. Spectra showing the wavelength region 6480 to 6510 Å, for the same stars as in Fig. 1.

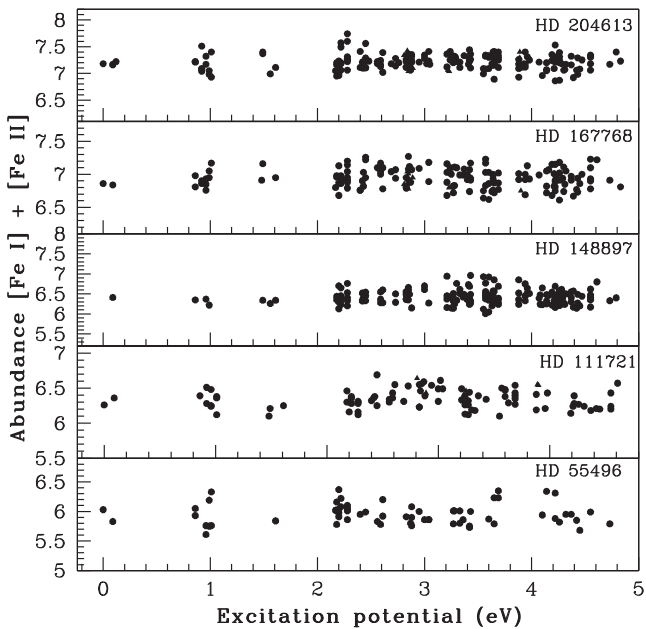


Figure 3. The iron abundances of stars are shown for individual Fe I and Fe II lines as a function of excitation potential. The solid circles indicate Fe I lines and solid triangles indicate Fe II lines.

Luck & Bond (1991), Sneden et al. (1996), and Kurucz atomic line data base (Kurucz 1995a,b). The log gf values for a few La lines are taken from Lawler, BonVallet & Sneden (2001). We have estimated abundances for many elements Na, Mg, Ca, Sc, Ti, V, Cr, Mn, Co, Ni, Zn and for heavy elements Sr, Y, Zr, Ba, La, Ce, Pr, Nd, Sm, Eu and Dy. For the elements Sc, V, Mn, Ba, La and Eu, spectrum synthesis is used to find the abundances considering hyperfine structure. The line lists for each region that is synthesized are taken from Kurucz atomic line list (<http://www.cfa.harvard.edu/amp/ampdata/kurucz23/sekur.html>). A few examples of spectrum synthesis calculations are shown in Figs 5, 6 and 7.

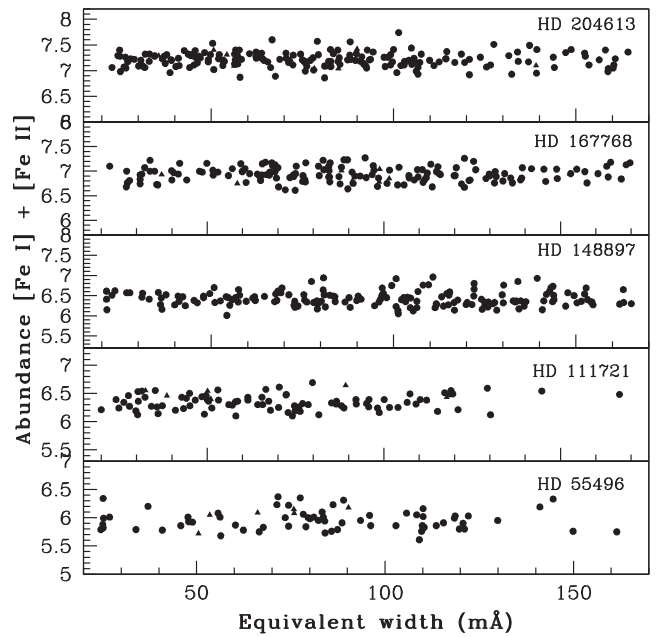


Figure 4. The iron abundances of stars are shown for individual Fe I and Fe II lines as a function of equivalent width. The solid circles indicate Fe I lines and solid triangles indicate Fe II lines.

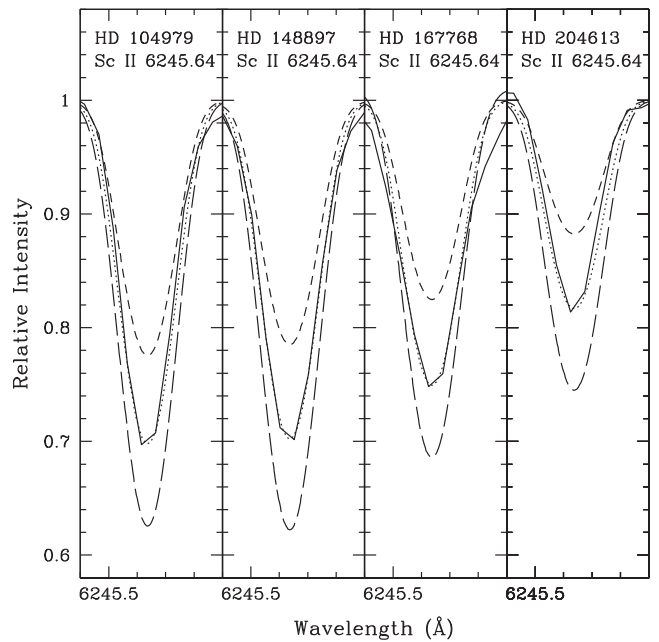


Figure 5. Spectral-synthesis fits of Sc II line at 6245.64 Å. The dotted lines indicate the synthesized spectra and the solid lines indicate the observed line profiles. Two alternative synthetic spectra for $[X/Fe] = +0.3$ (long-dashed line) and $[X/Fe] = -0.3$ (short-dashed line) are shown to demonstrate the sensitivity of the line strength to the abundances.

Derived abundance ratios with respect to iron are listed in Table 6. In Table 7, we have presented $[ls/Fe]$, $[hs/Fe]$ and $[hs/ls]$ values, where ls represents light s-process elements Sr, Y and Zr and hs represents heavy s-process elements Ba, La, Ce, Nd and Sm. Lines used for the abundance calculation of these elements are listed in Tables 8A, 8B, 9A and 9B.

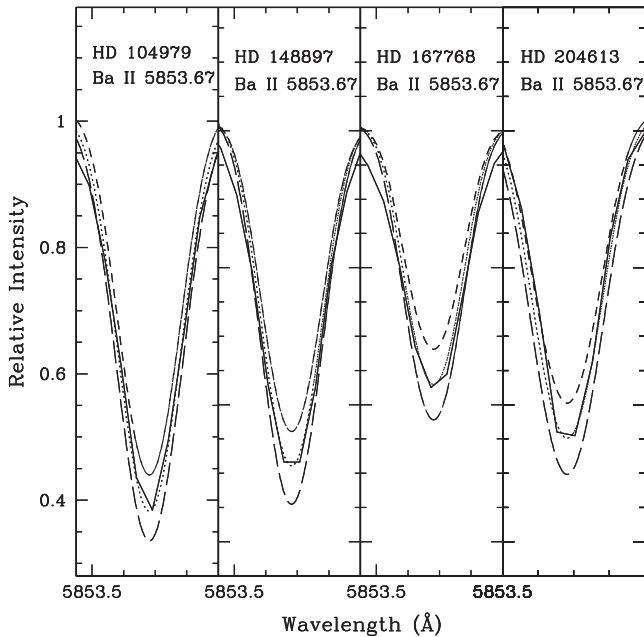


Figure 6. Spectral-synthesis fits of Ba II line at 5853.67 Å. The dotted lines indicate the synthesized spectra and the solid lines indicate the observed line profiles. Two alternative synthetic spectra for $[X/Fe] = +0.3$ (long-dashed line) and $[X/Fe] = -0.3$ (short-dashed line) are shown to demonstrate the sensitivity of the line strength to the abundances.

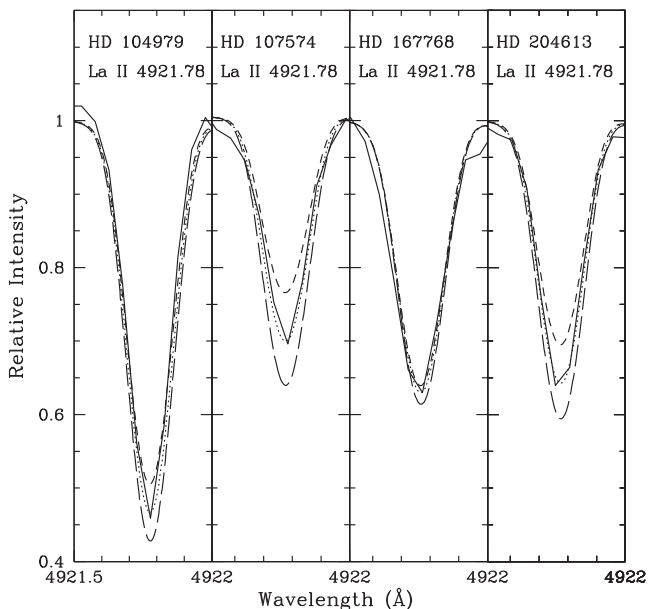


Figure 7. Spectral-synthesis fits of La II line at 4921.78 Å. The dotted lines indicate the synthesized spectra and the solid lines indicate the observed line profiles. Two alternative synthetic spectra for $[X/Fe] = +0.3$ (long-dashed line) and $[X/Fe] = -0.3$ (short-dashed line) are shown to demonstrate the sensitivity of the line strength to the abundances.

6.1 Carbon

We have derived the carbon abundance for our objects whenever possible using the spectrum synthesis calculation of C I line at 5380.337 Å. The line list is generated from Kurucz atomic and molecular line data base (<http://www.cfa.harvard.edu/amp/ampdata/kurucz23/sekur.html>). This line appears heavily distorted

in the spectra of stars HD 89668, HD 111721 and HD 126681 and hence C abundance could not be determined for these objects from this line. In the case of HD 148897, a very weak feature of C I at 5380.337 Å is detected; however, this line could not be used for abundance determination using the spectrum synthesis calculation. For the stars HD 148897 and HD 111721, the carbon abundance is determined using spectrum synthesis calculation of the CH band at 4300 Å. For HD 126681, we could not find C abundance due to severe line distortion and blending throughout the spectrum. Estimated $[C/Fe]$ ratios are listed in Table 6. We have derived the $^{12}C/^{13}C$ ratio for seven objects from spectrum synthesis of the CH band. The initial $^{12}C/^{13}C$ is fixed at solar value and then varied to fit the observed spectrum for the determined carbon abundances. The estimated values lie in the range 4–19 and are presented in Table 5 along with the atmospheric parameters. The line list for the synthesis of CH band is taken from the Kurucz data base for molecular lines. We have derived a $[C/H]$ value of -0.23 and -1.23 for two cyanogen weak giants HD 104979 and HD 148897. For these objects, Luck (1991) reported the $[C/H]$ values -0.38 and -0.94 , respectively. We have determined a carbon abundance of 8.68 dex for HD 204613 while Smith, Coleman & Lambert (1993) reported 8.91 dex for the same object. North, Berthet & Lanz (1994) have given the $[C/H]$ ratios -0.07 and -0.03 , respectively for HD 92545 and HD 107574. We have derived slightly lower $[C/H]$ values for these objects. For HD 92545 and HD 107574, our estimated $[C/H]$ values are -0.37 and -0.18 , respectively. Masseron et al. (2010) listed the $[C/Fe]$ ratio of these two objects as 0.32 and 0.39, respectively. Carbon abundance for HD 122202 is not available in the literature. We have derived -0.13 for $[C/H]$ and 0.5 for $[C/Fe]$ in this object. Our estimates of $[C/H] \sim 0.48$ and $[C/Fe] \sim 0.03$ in HD 167768 are in good agreement with the estimates of -0.63 and -0.02 respectively of Luck & Heiter (2007).

6.2 Na and Al

The abundance of sodium is derived for all the objects except HD 122202. For most of the objects, we have used the lines at 5682.65 and 5688.22 Å. We have also used the doublet lines at 5890.9 and 5895.9 Å for determination of sodium abundances. However, the resonance lines are sensitive to non-LTE effects. The observed LTE abundance ranges between -0.29 and 0.49 in the programme stars.

Even though we could measure a few Al lines in our programme stars spectra, these are not usable for abundance determination of Al.

6.3 Mg, Si, Ca, Sc, Ti, V

We have measured several lines due to these elements. Except for HD 92545 and HD 104979 that show near-solar values, all other stars show mild enhancement of Mg with $[Mg/Fe] \geq 0.15$. $[Mg/Fe]$ in HD 148897 with a metallicity of -1.02 is ~ 0.63 , slightly higher than as expected for classical enhancement of α -elements in stars with $[Fe/H] \sim -1.0$ (Goswami & Prantzos 2000). Abundance of Si could not be estimated as none of the Si lines are found usable for abundance determination. Ca shows a near-solar value in HD 92545, HD 104979, HD 126681 and HD 164922. In the rest of the objects, Ca is found to be mildly enhanced.

Sc abundance is determined using spectrum synthesis calculation of Sc II line at 6245.63 Å considering hyperfine structure from Prochaska & McWilliam (2000). We could determine Sc abundance in seven of the programme stars. Except HD 204613 with $[Sc/Fe]$ value 0.17, all the other objects show mild underabundance of Sc.

Table 6. Elemental abundances.

Star name	[C/Fe]	[Na I/Fe]	[Mg I/Fe]	[Ca I/Fe]	[Sc II/Fe]	[Ti I/Fe]	[Ti II/Fe]	[V I/Fe]	[Cr I/Fe]	[Cr II/Fe]	[Mn I/Fe]	[Co I/Fe]	[Ni I/Fe]	[Zn I/Fe]
Sub-giant														
CH stars														
HD 122202	0.50	–	0.32	0.33	–	–	0.36	–	0.11	–	–	–	0.14	0.59
HD 204613	0.49	0.08	0.11	0.13	0.17	0.26	0.41	–0.01	–0.06	0.08	–0.33	–0.19	0.04	–
#CH stars														
*HD 55496	1.01	0.4	0.33	0.46	–	–0.1	–0.16	0.19	–0.35	–0.21	–	–	–0.18	0.02
HD 89668	0.05	0.08	0.28	0.63	0.0	–0.26	–0.38	–	–0.09	–0.27	0.34	–0.23	–0.12	–
HD 92545	0.68	0.01	–0.09	–0.05	–	0.03	0.6	–	–0.15	–	–	0.8	0.01	–
HD 104979	0.03	–0.01	0.07	0.05	–0.01	0.14	0.32	0.05	–0.02	0.06	–0.23	0.28	0.04	–0.03
HD 107574	0.47	0.49	–	0.19	–0.13	0.32	0.34	–	0.1	–0.26	–	–	0.01	–
HD 111721	0.08	0.07	0.46	0.41	–	0.46	0.03	–	–0.21	–0.31	–	–	–0.07	–
HD 126681	–	–0.26	0.44	0.07	–	0.52	0.60	–	0.1	–	–	–	–0.08	–
HD 148897	–0.21	–0.29	0.63	0.19	–0.33	0.11	0.46	–0.18	–0.22	0.0	–0.54	0.06	–0.13	–0.26
HD 164922	–0.15	–0.02	0.36	–0.07	–0.47	0.25	0.05	0.40	0.04	0.06	0.14	0.13	0.06	0.19
HD 167768	0.03	0.04	0.17	0.22	–0.04	0.17	0.41	0.2	–0.09	–0.21	–0.56	–0.03	–0.09	0.18
Star name	[Sr I/Fe]	[Y II/Fe]	[Zr II/Fe]	[Ba II/Fe]	[La II/Fe]	[Ce II/Fe]	[Pr II/Fe]	[Nd II/Fe]	[Sm II/Fe]	[Eu II/Fe]	[Dy II/Fe]			
Sub-giant														
CH stars														
HD 122202	–	1.44	–	0.33	0.9	1.62	1.26	–	1.77	–	–			
HD 204613	1.71	0.97	1.14	1.04	1.21	1.24	1.52	1.02	1.61	0.06	1.77			
#CH stars														
*HD 55496	0.82	0.85	0.52	0.57	–	0.13	0.43	–	–	–	–			
HD 89668	1.06	0.55	–	–0.24	1.87	1.52	1.66	1.44	1.23	0.38	–			
HD 92545	–	0.23	–	0.91	0.95	1.6	–	–	–	–	–			
HD 104979	0.99	0.71	0.85	0.94	1.11	1.06	1.04	1.13	1.17	0.40	–			
HD 107574	–	1.02	–	0.97	1.04	0.6	–	–	–	–	–			
HD 111721	–	0.05	–	–0.09	0.31	1.6	–	2.1	–	–	–			
HD 126681	–	0.02	–	0.27	–	0.67	–	1.2	1.07	–	–			
HD 148897	0.31	0.03	–0.47	–0.65	0.29	–0.16	–	0.13	0.58	–	0.02			
HD 164922	0.79	0.14	–	0.28	0.15	–0.09	–	–	–	–	–			
HD 167768	0.77	0.56	0.2	–0.36	–0.54	0.06	–	0.65	0.9	0.26	1.04			

Notes: #Objects from the CH star catalogue of Bartkevicius (1996).

*Objects are also included in Ba star catalogue of Lü (1991).

Table 7. Observed values for [Fe/H], [ls/Fe], [hs/Fe] and [hs/ls].

Star name	[Fe/H]	[ls/Fe]	[hs/Fe]	[hs/ls]	Remarks
HD 55496	–1.49	0.73	0.38	–0.35	1
HD 89668	–0.13	0.81	1.16	0.35	1
HD 92545	–0.21	0.23	1.15	0.92	1
HD 104979	–0.26	0.85	1.03	0.18	1
HD 104979	–0.47	0.6	1.0	0.4	2
HD 107574	–0.48	1.02	0.87	–0.15	1
HD 111721	–1.11	0.05	0.98	0.93	1
HD 122202	–0.63	1.44	1.16	–0.28	1
HD 126681	–0.90	0.02	0.80	0.78	1
HD 148897	–1.02	–0.13	0.01	0.14	1
HD 164922	0.22	0.47	0.10	–0.37	1
HD 167768	–0.51	0.51	0.14	–0.37	1
HD 204613	–0.24	1.27	1.16	–0.11	1
HD 204613	–0.35	1.0	0.6	–0.4	2

Notes: 1. Our work; 2. Busso et al. (2001).

Mild overabundance or near-solar abundance for Ti is noticed in all the programme stars except for HD 89668 and HD 92545. More than 10 good lines of Ti are used for abundance determination.

Abundance of V is estimated from spectrum synthesis calculation of V I line at 5727.028 Å taking into account the hyperfine components from Kurucz data base. We could determine V abundance only in six objects. While HD 148897 shows a mild under abun-

dance with [V/Fe] \approx –0.18, HD 89668, HD 104979, HD 167768, and HD 204613 show near-solar values. HD 164922 shows a mild overabundance with [V/Fe] = 0.40. We have detected more than 16 V I lines but only one or two are usable for the determination of abundance; other lines appear either blended or distorted in the spectra.

6.4 Cr, Co, Mn, Ni, Zn

HD 122202, HD 107574, HD 148897 and HD 164922 show a near-solar abundance for Cr. The rest of the stars in our sample are mildly underabundant in Cr. HD 55496 however shows a larger underabundance with [Cr/Fe] = –0.35. Cr abundances measured using Cr II lines whenever possible also show similar trends.

Mn abundance is obtained using spectrum synthesis calculation of 6013.51 Å line taking into account the hyperfine structures from Prochaska & McWilliam (2000). Except for HD 89668 and HD 164922, that show a mild overabundance with [Mn/Fe] \sim 0.34 and 0.14, respectively, the rest of the objects show underabundance with [Mn/Fe] \leq –0.23.

Except HD 92545 with [Co/Fe] \sim 0.80, all other stars in our sample show near-solar values or mild underabundance for Co.

Abundances of Ni measured from Ni I lines give near-solar values for all the stars.

HD 122202 is mildly overabundant in Zn with [Zn/Fe] = 0.59. The rest of the objects show near-solar values.

Table 8A. Equivalent widths in mÅ of lines used for the calculation of light element abundances for first six objects.

Wavelength (Å)	Element	$E_{\text{low}}(\text{ev})$	$\log gf$	HD 55496	HD 89668	HD 92545	HD 104979	HD 107574	HD 111721
5682.650	Na I	2.100	-0.700	58.07	208.7	63.7	115.9	50.1	-
5688.220		2.100	-0.400	-	205.3	89.9	131.6	-	29.9
5889.950		0.000	0.100	275.5	-	-	450.2	253.8	263.3
5895.920	Mg I	0.000	-0.200	-	-	225.4	379.5	226.1	245.6
4702.990		4.350	-0.666	103.2	-	172.8	188.9	-	143.1
6318.720		5.108	-1.730	15.88	86.1	82.6	137.4	-	79.4
5528.000		4.350	-0.490	142.3	-	162.6	202.4	-	139.0
4098.500	Ca I	2.525	-0.540	-	-	-	-	-	-

Note: This table is available in its entirety in online only. A portion is shown here for guidance regarding its form and content.

Table 8B. Equivalent widths in mÅ of lines used for the calculation of light element abundances for next six objects.

Wavelength (Å)	Element	$E_{\text{low}}(\text{ev})$	$\log gf$	HD 122202	HD 126681	HD 148897	HD 164922	HD 167768	HD 204613
5682.650	Na I	2.100	-0.700	-	22.8	73.7	137.6	93.2	87.5
5688.220		2.100	-0.400	-	-	93.0	143.4	118.7	106.2
5889.950		0.000	0.100	-	263.2	396.5	-	379.1	377.3
5895.920	Mg I	0.000	-0.200	-	234.5	340.2	601.4	329.7	-
4702.990		4.350	-0.666	147.3	-	186.2	334.3	182.4	232.6
6318.720		5.108	-1.730	-	60.7	35.3	133.2	35.5	88.3
5528.000		4.350	-0.490	-	156.7	212.2	320	205.3	201.8
4098.500	Ca I	2.525	-0.540	-	-	-	130.6	-	79.2

Note: This table is available in its entirety in online only. A portion is shown here for guidance regarding its form and content.

Table 9A. Equivalent widths in mÅ of lines used for abundance determination of heavy elements for the first six objects.

Wavelength (Å)	Element	$E_{\text{low}}(\text{ev})$	$\log gf$	HD 55496	HD 89668	HD 92545	HD 104979	HD 107574	HD 111721
4607.327	Sr I	0.000	-0.570	36.42	140.9	-	91.55	-	-
4854.863		0.992	-0.380	-	90.5	57.6	120.6	-	-
4883.685	Y II	1.084	0.070	-	74.4	89.9	121.2	106.8	51.7
5087.416		1.080	-0.170	103.5	-	72.1	91.82	-	56.2
5119.112		0.992	-1.360	41.16	-	27.4	55.28	-	-
5205.724		1.033	-0.340	42.89	-	-	-	-	-
5289.815	Y II	1.033	-1.850	27.11	-	-	33.81	-	-
5544.611		1.738	-1.090	-	-	-	36.53	-	-

Note: This table is available in its entirety in online only. A portion is shown here for guidance regarding its form and content.

Table 9B. Equivalent widths in mÅ of lines used for abundance determination of heavy elements for the next six objects.

Wavelength (Å)	Element	$E_{\text{low}}(\text{ev})$	$\log gf$	HD 122202	HD 126681	HD 148897	HD 164922	HD 167768	HD 204613
4607.327	Sr I	0.000	-0.570	-	-	89.9	58.5	68.6	77.31
4854.863		0.992	-0.380	-	-	98.6	53.8	72.2	82.63
4883.685	Y II	1.084	0.070	129.5	28.6	114.5	-	80.6	101.4
5087.416		1.080	-0.170	-	23.8	82.3	40.5	66.1	86.53
5119.112		0.992	-1.360	-	-	41.6	19.0	16.2	47.09
5205.724		1.033	-0.340	-	-	-	-	-	92.26
5289.815	Y II	1.033	-1.850	-	-	-	-	14.2	15.22
5544.611		1.738	-1.090	-	-	18.6	-	11.7	29.54

Note: This table is available in its entirety in online only. A portion is shown here for guidance regarding its form and content.

6.5 Sr, Y, Zr

The abundance of Sr is estimated in seven stars using Sr I line at 4607.327 Å. Sr is overabundant in HD 89668 and HD 204613 with $[\text{Sr}/\text{Fe}] > 1.0$. The other five objects HD 55496, HD 104979, HD 148897, HD 164922 and HD 167768 give $[\text{Sr}/\text{Fe}]$ ratios in the range 0.30–0.99. Abundance of Sr could not be estimated in the remaining objects as the line at 4607.327 Å appears distorted in their spectra.

None of the Sr II lines detected are found suitable for abundance estimate of Sr.

The abundance of Y is measured in all the stars. Y is overabundant in HD 122202 and HD 107574 with $[\text{Y}/\text{Fe}]$ ratio ≥ 1.0 . HD 204613 and HD 55496 show $[\text{Y}/\text{Fe}]$ values of 0.97 and 0.85, respectively. The remaining stars show near-solar values or mild overabundance.

Table 10. Atmospheric parameters from literature.

Star name	Vmag	T_{eff} (K)	log g	[Fe/H]	Reference		
HD 55496	8.40	4850	2.05	-1.45	1		
		4858	2.05	-1.48	2		
		4935	2.33	-1.44	3		
		4800	2.8	-1.55	4		
HD 89968	9.41	5400	4.35	-0.13	1		
		4811	4.45	-0.11	5		
HD 92545	8.56	6380	4.65	-0.21	1		
		6240	4.23	-0.26	6		
HD 104979	4.13	5060	2.67	-0.26	1		
		4842	2.9	-0.51	7		
		4996	2.86	-0.33	8		
		4825	2.34	-0.33	9		
		4870	3.23	-0.51	10		
		4893	2.6	-0.29	11		
		4990	2.65	-0.11	12		
		5250	3.25	-0.29	13		
		HD 107544	8.55	6250	2.9	-0.65	1
				6340	3.87	-0.36	6
		HD 111721	7.97	5212	2.6	-1.11	1
5120	2.90			-1.27	3		
4995	2.52			-1.26	14		
4825	2.2			-1.54	15		
4800	3.00			-1.68	16		
5164	3.27			-0.98	17		
4940	2.40			-1.34	18		
5103	3.06			-1.22	19		
5000				-1.34	20		
5103	2.87			-1.25	21		
HD 122202	9.37	6430	4.0	-0.63	1		
		6600	3.0	-0.09	4		
HD 126681	9.32	5760	4.65	-0.90	1		
		5507	4.45	-1.17	22		
		5561	4.71	-1.14	5		
		5577	4.25	-1.12	2		
		5475	4.65	-1.38	23		
		5533	4.28	-1.14	24		
		5450	4.5	-1.25	15		
		5595	4.43	-1.12	22		
		5625	4.95	-1.09	17		
		5500	4.63	-1.45	25		
HD 148897	5.25	4285	0.6	-1.02	1		
		4293	1.01	-1.11	2		
		4100	0.09	-1.16	4		
		4345	1.5	-0.62	26		
HD 167768	6.00	5070	2.55	-0.51	1		
		4953	2.29	-0.69	2		
		5102	2.76	-0.61	8		
HD 204613	8.21	5875	4.2	-0.24	1		
		5718	3.88	-0.38	2		
		5650	3.80	-0.35	27		
		5650	3.80	-0.35	28		
		5600	3.5	-0.70	29		
		5600	3.5	-0.65	30		
		5663	3.75	-0.54	31		

References. 1. Our work 2. Prugniel, Vauglin & Koleva (2011), 3. Koleva & Vazdekis (2012), 4. Luck & Bond (1991), 5. Sousa et al. (2011), 6. North et al. (1994), 7. Massarotti et al. (2008), 8. Luck & Heiter (2007), 9. Luck (1991), 10. McWilliam (1990), 11. Tomkin & Lambert (1986), 12. Sneden, Lambert & Pilachowski (1981), 13. Lambert & Ries (1981), 14. Gratton et al. (2000), 15. Fulbright (2000), 16. Cavallo, Pilachowski & Rebolo (1997), 17. Gratton, Carretta & Castelli (1996), 18. Ryan & Lambert (1995), 19. Gratton & Sneden (1994), 20. Pilachowski, Sneden & Booth (1993), 21. Gratton & Sneden (1991), 22. Nissen & Schuster (2011), 23. Sozzetti et al. (2009), 24. Nissen et al. (2000), 25. Tomkin et al. (1992), 26. Kyrolainen et al. (1986), 27. Frasca et al. (2009), 28. Smith et al. (1993), 29. Rebolo, Molaro & Beckman (1988), 30. Abia et al. (1988), 31. Smith & Lambert (1986).

We could derive Zr abundance for five stars. HD 204613 and HD 104979 show overabundance with [Zr/Fe] values 1.14 and 0.85, respectively. The rest show mild enhancement with [Zr/Fe] ≥ 0.2 .

6.6 Ba, La, Ce, Pr, Nd, Sm, Eu, Dy

As many lines due to Ce, Pr, Nd, Sm and Dy could be measured on our spectra, the standard abundance determination method using equivalent width measurements are used for abundance estimates. Spectrum synthesis calculation is also performed for Ba, La and Eu. We have estimated the abundance for Ba and Ce in all the stars.

Barium (Ba): we have determined Ba abundance from spectrum synthesis calculation using Ba II line at 5853.668 Å considering hyperfine components from McWilliam (1998). Four stars in our sample HD 92545, HD 104979, HD 107574 and HD 204613 show overabundance with [Ba/Fe] ≥ 0.9 . HD 122202, HD 55496 and HD 126681 show only a mild overabundance. Four objects, HD 89668, HD 111721, HD 148897 and HD 167768 show underabundance with [Ba/Fe] in the range -0.09 to -0.65 (Table 6).

Lanthanum (La): we have derived La abundance for all the programme stars except for HD 55496 and HD 126681 from spectrum synthesis calculation of La II line at 4921.77 Å considering hyperfine components from Jonsell et al. (2006). Except for HD 111721, HD 148897, HD 164922 and HD 167768, La in all other stars are found to be overabundant with [La/Fe] ≥ 0.9 . HD 111721, HD 148897, HD 164922 and HD 167768 show [La/Fe] of 0.31, 0.29, 0.15 and -0.54, respectively.

Cerium (Ce): we have derived Ce abundance for all the programme stars. Six of the programme stars, HD 89668, HD 92545, HD 104979, HD 111721, HD 122202 and HD 204613 show overabundance with [Ce/Fe] ≥ 1.0 . Estimated [Ce/Fe] for HD 107574 is ~ 0.6 . While two stars HD 55496 and HD 167768 show almost near-solar values for [Ce/Fe], HD 148897 and HD 164922 show mild underabundance with [Ce/Fe] ≈ -0.10 .

Praseodymium (Pr): we could derive Pr abundance for five programme stars mainly using the Pr II line at 5292.619 Å. A mild overenhancement of Pr is seen in HD 55496 with [Pr/Fe] ~ 0.43 ; the rest show overabundance with [Pr/Fe] ≥ 1.0 .

Neodymium (Nd): abundance of Nd is estimated for seven programme stars. Two stars HD 148897 and HD 167768 give [Nd/Fe] values ~ 0.13 and 0.65, respectively. HD 111721 shows a large overabundance with [Nd/Fe] ~ 2.1 . All other stars show overabundance with [Nd/Fe] ≥ 1.0 .

Samarium (Sm): HD 148897 shows a mild overabundance with [Sm/Fe] ~ 0.58 . HD 89668, HD 104979, HD 122202, HD 126681 and HD 204613 show overabundance with [Sm/Fe] ≥ 1.0 . Estimated [Sm/Fe] in HD 167768 is ~ 0.90 .

Europium (Eu): we could determine Eu abundance in four of the programme stars using spectrum synthesis of Eu II lines at 6645.130 Å by considering the hyperfine components from Worley et al. (2013). Eu shows mild overabundance in HD 89668, HD 92545 and HD 167768 with [Eu/Fe] ~ 0.38 , 0.40 and 0.26, respectively. HD 204613 shows a near-solar value with [Eu/Fe] ~ 0.06 .

Dysprosium (Dy): we could derive Dy abundance for three objects HD 148897, HD 167768 and HD 204613 using Dy II lines at 4103.310 and 4923.167 Å. HD 167768 and HD 204613 show overabundance with [Dy/Fe] ≥ 1.0 . HD 148897 shows a near-solar value of ~ 0.02 .

Table 11. Comparison of our results with literature values.

Star name	[Sr μ /Fe]	[Y μ /Fe]	[Zr μ /Fe]	[Ba μ /Fe]	[La μ /Fe]	[Ce μ /Fe]	[Pr μ /Fe]	[Nd μ /Fe]	[Sm μ /Fe]	[Eu μ /Fe]	[Dy μ /Fe]	References
Sub-giant CH stars												
HD 122202	–	1.44	–	0.33	0.9	1.62	1.26	–	1.77	–	–	1
	–	0.74	0.15	–	0.79	0.74	–	0.75	0.44	–	–	2
HD 204613	1.71	0.97	1.14	1.04	1.21	1.24	1.52	1.02	1.61	0.06	1.77	1
	–	1.22	1.00	0.71	–	–	–	0.77	–	–	–	3
#CH stars												
HD 55496	0.82	0.85	0.52	0.57	–	0.13	0.43	–	–	–	–	1
	–	–	0.72	–	0.52	0.32	–	0.52	0.33	–	–	2
HD 89968	1.06	0.55	–	–0.24	1.87	1.52	1.66	1.44	1.23	0.38	–	1
HD 92545	–	0.23	–	0.91	0.95	1.6	–	–	–	–	–	1
	0.67	0.64	0.75	1.04	0.72	0.60	0.44	0.42	0.24	0.32	0.09	4
HD 104979	0.99	0.71	0.85	0.94	1.11	1.06	1.04	1.13	1.17	0.40	–	1
	–	0.52	0.40	–	–	0.48	–	0.82	0.51	0.61	–	5
HD 107574	–	1.02	–	0.97	1.04	0.6	–	–	–	–	–	1
	0.67	0.64	0.75	1.04	0.72	0.6	0.44	0.42	0.24	0.14	0.09	4
HD 111721	–	0.05	–	–0.09	0.31	1.6	–	2.1	–	–	–	1
	–0.13	0.14	–0.45	0.08	0.04	0.03	0.28	0.17	0.22	0.36	–	6
	–	0.02	–	0.27	–	0.67	–	1.2	1.07	–	–	1
HD 126681	–	0.23	–	0.14	–	–	–	–	–	–	–	7
HD 148897	0.31	0.03	–0.47	–0.65	0.29	–0.16	–	0.13	0.58	–	0.02	1
	–	0.04	–0.29	–	–	0.07	–	0.01	–	–0.13	–	5
HD 164922	0.79	0.14	–	0.28	–	–0.09	–	–	–	–	–	1
	–	–0.15	0.04	–0.10	–	0.08	–	0.03	0.01	0.10	–	
HD 167768	0.77	0.56	0.2	–0.36	–0.54	0.06	–	0.65	0.9	0.26	1.04	1
	–	0.03	–	–0.03	–	–0.04	–0.10	–0.14	–	0.45	–	8

Notes: #Objects from the CH star catalogue of Bartkevicius (1996)

*Objects are also included in Ba star catalogue of Lü (1991)

1. Our work 2. Luck & Bond (1991) 3. Smith et al. (1993) 4. Allen & Barbuy (2006a) 5. Luck (1991) 6. Gratton & Sneden (1994) 7. Fulbright (2000) 8. Luck & Heiter (2007).

7 DISCUSSION ON INDIVIDUAL STARS

Comparisons of our estimated atmospheric parameters and elemental abundance ratios with literature values whenever available, are presented in Tables 10 and 11 respectively. *HD 55496*: Bond (1974) has classified this high-velocity object as a sub-giant CH star. MacConnell (1972) included this in the category of weak lined metal-deficient Ba II star. Being a high-velocity object with lower metallicity, $\langle [\text{Fe}/\text{H}] = -1.45$ *HD 55496* seems to show the extreme halo kinematics. Luck & Bond (1991) have studied this object and reported abundances for a few elements (Table 11). Estimated Ba abundance ($[\text{Ba}/\text{Fe}] = 0.57$) does not qualify the object to be a typical CH star. Light s-process elements Sr, Y and Zr are more abundant in this star than the heavy s-process elements Ba, Ce, and Pr.

HD 89668: we present first time detailed abundances for this object. This object shows large enhancements in La, Ce, Pr, Nd and Sm with $[X/\text{Fe}]$ values ≥ 1 ; however, Ba is slightly underabundant with $[\text{Ba}/\text{Fe}] \sim -0.24$.

HD 92545, *HD 107574*: North & Duquennoy (1991) have categorized these objects as F str Lambda 4077 stars following the classification of Bidelman (1981). Allen & Barbuy (2006a,b) have reported detailed chemical abundances for these objects (Table 11). For *HD 92545*, our Ce abundance is higher than their estimates. Other elements show a close similarity and within the error limits. For *HD 107574*, our results are fairly in good agreement with their estimates.

HD 104979, *HD 148897*: Luck (1991) identified these objects as cyanogen weak giants and reported elemental abundances for Y, Zr, Ce, Nd and Eu. Our results closely match with their values. In

addition to these elements, we could measure abundances for Sr, Ba, La, Sm, Pr and Dy. Similar to the two cyanogen weak giants *HD 188650* and *HD 214714* from our Paper I, the object *HD 148897* also does not show large enhancement in heavy elements. These three objects are of the same spectral type. The object *HD 104979* shows enhancements in Ba with $[\text{Ba}/\text{Fe}] = 0.94$. Estimated metallicities of these objects are in the range -0.2 to -1.2 .

HD 111721: Gratton & Sneden (1994) have studied this object and reported abundances for heavy elements. From our analysis and also from Gratton & Sneden (1994), this object does not show enhancement in heavy elements. The metallicity of this object is -1.11 . This object could be a possible member of the group of CEMP-no stars of Beers & Christlieb's (2005) carbon star classification scheme.

HD 122202, *HD 204613*: these two objects are CH sub-giants. Luck & Bond (1991) have studied the object *HD 122202* and reported abundances for a few s-process elements. *HD 204613* was studied by Smith (1984); these authors gave the abundances for Y, Zr, Ba and Nd in this object. In addition to these elements, we estimated the abundances for Sr, La, Ce, Pr, Sm, Eu and Dy in *HD 204613* and La, Pr and Sm in *HD 122202*. The object *HD 122202* shows a large enhancement in Ce, Pr and Nd. However, Ba is only mildly enhanced with $[\text{Ba}/\text{Fe}] \sim 0.33$. *HD 204613* shows a large enhancement in all the elements except Eu. According to Beers & Christlieb (2005) classification, this object fall in to the group of CEMP-s stars with $[\text{Ba}/\text{Fe}] \sim 1.04$ and $[\text{Ba}/\text{Eu}] \sim 0.98$. McClure (1997) have confirmed these objects as binaries. Information on radial velocity variability and orbital elements for these objects are available in McClure (1997). While *HD 122202* shows radial velocity variations in the range -14.81 to -7.64 with an orbital period

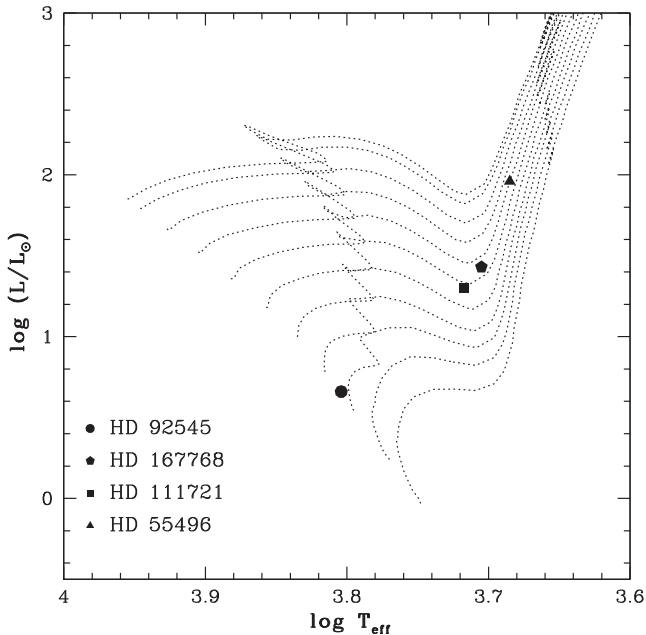


Figure 8. The location of HD 92545, HD 167768, HD 111721 and HD 55496 are indicated in the H–R diagram. The masses are derived using the evolutionary tracks of Girardi et al. (2000). The evolutionary tracks for masses 1, 1.1, 1.2, 1.3 1.4, 1.5, 1.6 1.7, 1.8, 1.9 and 1.95 M_{\odot} from bottom to top are shown in the figure.

of 1290 ± 9 d; HD 204613 exhibits radial velocity variations from -95.07 to -87.85 with period 878 ± 4 d.

HD 126681: we have presented the first time abundance estimates for the elements Ce, Nd and Sm in this object. Fulbright (2000) has studied this object and reported abundances for Y and Ba. This object shows a large enhancement in Nd and Sm but other heavy elements are only mildly enhanced.

HD 164922: the object HD 164922 is listed as a CH star by many authors, however, this object does not seem to show any characteristics of CH stars. Mishenina et al. (2013) have studied this object and reported abundances for a few heavy elements that show almost near-solar values for Zr, Ba, Ce, Nd, Sm and Eu. Our estimated Ba and Ce abundances give $[\text{Ba}/\text{Fe}] \sim 0.28$ and $[\text{Ce}/\text{Fe}] \sim -0.09$ for this object.

HD 167768: Luck & Heiter (2007) have studied this object and reported abundances for Y, Ba, Ce, Pr, Nd, Eu. Along with these elements, we have estimated abundances for Sr, Zr, La and Sm. This object does not show large enhancement of heavy elements, a characteristic of CH stars.

8 STELLAR MASSES

We could estimate the stellar masses for eight objects in our sample from their locations in the Hertzsprung–Russel diagram (Figs 8 and 9), using the evolutionary tracks (Girardi et al. 2000) in the mass range of 0.15 – $7.0 M_{\odot}$ and the Z values from 0.0004 to 0.03. These evolutionary tracks are available at <http://pleiadi.pd.astro.it/>. For the objects with near-solar metallicity, we have selected an initial composition of $Z = 0.0198$, $Y = 0.273$. The masses derived using spectroscopic temperature estimates are presented in Table 12. For six stars in our sample that have metallicities < -0.5 , we used the evolutionary tracks corresponding to $Z = 0.008$. It is to be noted that the values of the masses obtained for these objects with $Z = 0.008$ are found to be similar to those obtained using evolutionary tracks

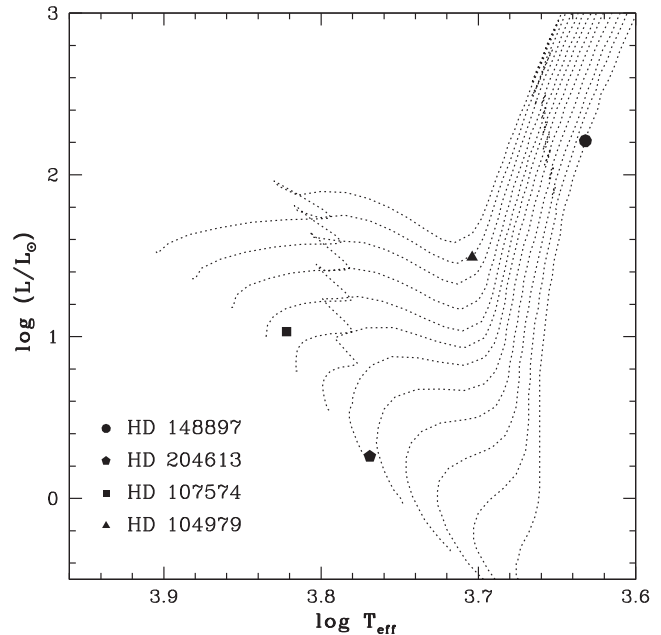


Figure 9. The location of HD 148897, HD 204613, HD 107574 and HD 104979 are indicated in the H–R diagram. The masses are derived using the evolutionary tracks of Girardi et al. (2000). The evolutionary tracks are shown for masses 0.6, 0.7, 0.8, 0.9, 1.0, 1.1, 1.2, 1.3 1.4, 1.5, 1.6 1.7, 1.8, 1.9 and 1.95 M_{\odot} from bottom to top.

Table 12. Stellar masses.

Star name	M_v	$\log(L/L_{\odot})$	Mass(M_{\odot})
HD 55496	-0.16	1.96	1.6
HD 92545	3.1	0.66	1.2
HD 104979	0.63	1.49	1.6
HD 107574	2.1	1.03	1.45
HD 111721	1.2	1.3	1.5
HD 148897	2.3	2.21	0.60
HD 167768	2.1	1.43	1.55
HD 204613	3.9	0.26	1.1

corresponding to $Z = 0.019$. Derived stellar masses are in the range 0.6 – $1.6 M_{\odot}$ with HD 55496 having a mass of $1.6 M_{\odot}$ and HD 148897 $\sim 0.6 M_{\odot}$. Stellar masses could not be estimated for the rest of the objects as the parallax estimates are not available in the literature.

9 PARAMETRIC-MODEL-BASED STUDY

Elements heavier than iron are mainly produced by two neutron-capture processes, the s-process and the r-process. Observed abundances of heavy elements estimated using model atmospheres and spectral-synthesis techniques do not provide direct quantitative estimates of the relative contributions from s- and/or r- process nucleosynthesis. Identification of the dominant processes contributing to the heavy element abundances in the stars is likely to provide clues to their origin. We have investigated ways to delineate the observed abundances into their respective r- and s-process contributions in the framework of a parametric model using an appropriate model function. The origin of the n-capture elements is explored by comparing the observed abundances with predicted s- and r-process contributions following Goswami, Subramania Athiray &

Table 13. Best-fitting coefficients and reduced chi-square values.

Star name	A_s	A_r	χ^2
HD 92545	0.560 ± 0.33	0.503 ± 0.33	2.15
HD 104979	0.514 ± 0.16	0.493 ± 0.15	0.50
HD 107574	0.823 ± 0.01	0.171 ± 0.01	1.22
HD 204613	0.739 ± 0.08	0.291 ± 0.08	1.65

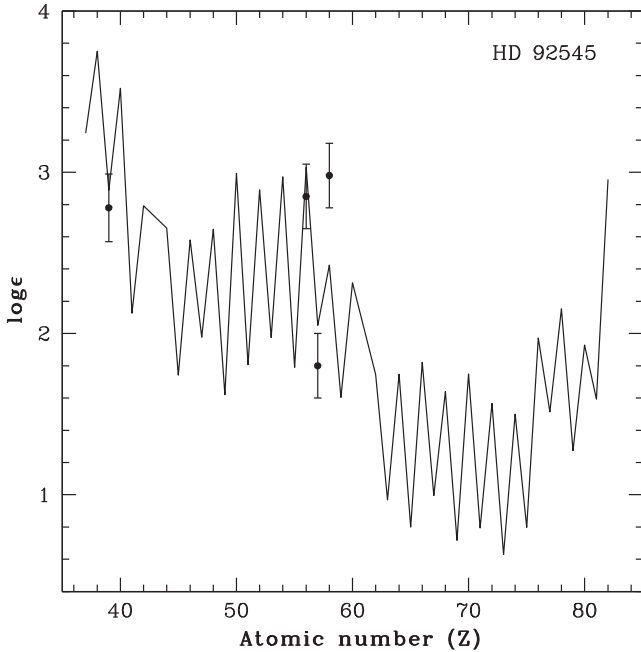


Figure 10. Solid curve represent the best fit for the parametric model function $\log \epsilon = A_s N_{si} + A_r N_{ri}$, where N_{si} and N_{ri} represent the abundances due to s- and r-process, respectively (Arlandini et al. 1999, Stellar model, scaled to the metallicity of the star). The points with error bars indicate the observed abundances in HD 92545.

Karinkuzhi (2010b, and references there in). The i th element abundance can be calculated as

$$N_i(Z) = A_s N_{is} + A_r N_{ir} 10^{[Fe/H]},$$

where Z is the metallicity of the star, N_{is} indicates the abundance from s-process in AGB star, N_{ir} indicates the abundance from r-process; A_s indicates the component coefficient that correspond to contributions from the s-process and A_r indicates the component coefficient that correspond to contributions from the r-process.

We have utilized the Solar system s- and r-process isotopic abundances from stellar models of Arlandini et al. (1999). The observed elemental abundances are scaled to the metallicity of the corresponding CH star and are normalized to their respective Ba abundances. Elemental abundances are then fitted with the parametric model function. The best-fitting coefficients and reduced chi-square values for a set of CH stars are given in Table 13. The best fits obtained with the parametric model function $\log \epsilon_i = A_s N_{is} + A_r N_{ir}$ for HD 92545, HD 104979, HD 107574 and HD 204613 are shown in Figs 10–13. The errors in the derived abundances play an important role in deciding the goodness of fit of the parametric model functions. From the parametric model based analysis, we find the objects HD 92545, HD 104979, HD 107574 and HD 204613 to belong to the group of CEMP-s stars.

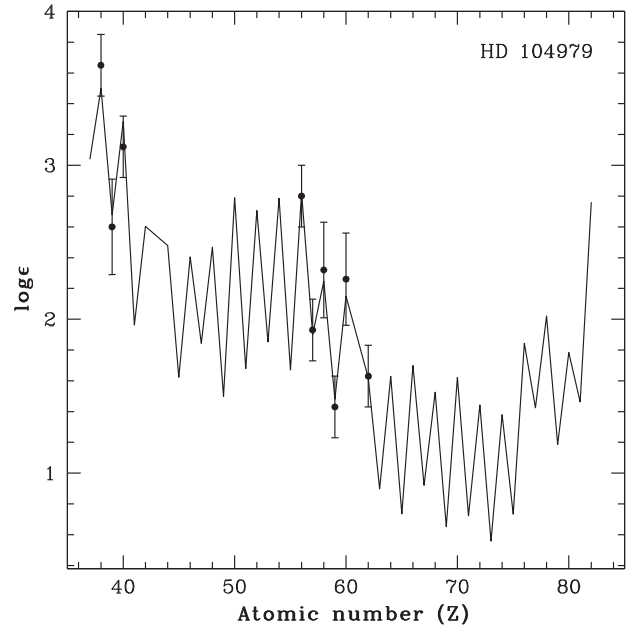


Figure 11. Solid curve represent the best fit for the parametric model function $\log \epsilon = A_s N_{si} + A_r N_{ri}$, where N_{si} and N_{ri} represent the abundances due to s- and r-process, respectively (Arlandini et al. 1999, Stellar model, scaled to the metallicity of the star). The points with error bars indicate the observed abundances in HD 104979.

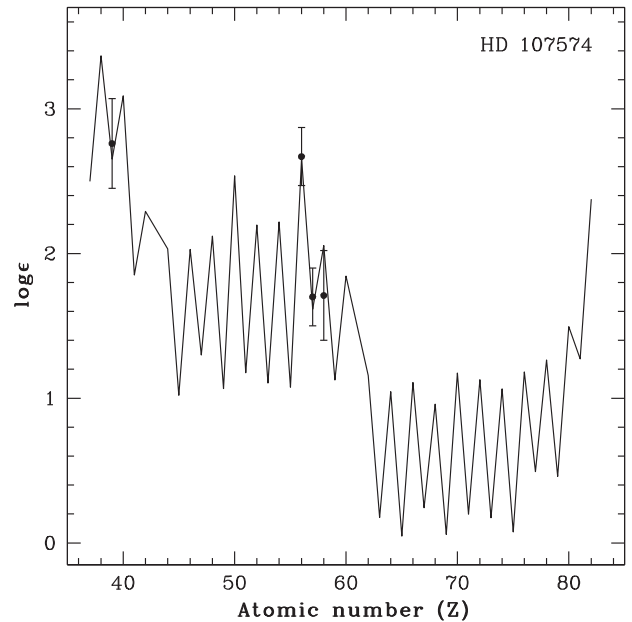


Figure 12. Solid curve represent the best fit for the parametric model function $\log \epsilon = A_s N_{si} + A_r N_{ri}$, where N_{si} and N_{ri} represent the abundances due to s- and r-process, respectively (Arlandini et al. 1999, Stellar model, scaled to the metallicity of the star). The points with error bars indicate the observed abundances in HD 107574.

10 CONCLUSION

Results from our analyses of a group of 12 stars from the CH star catalogue of Bartkevicius (1996) are presented. Abundances for 22 elements are estimated. Except for HD 55496 with radial velocity 315.2 Km s^{-1} , the rest are low-velocity objects. HD 55496 is also listed in the Ba star catalogue of Lü (1991). This object

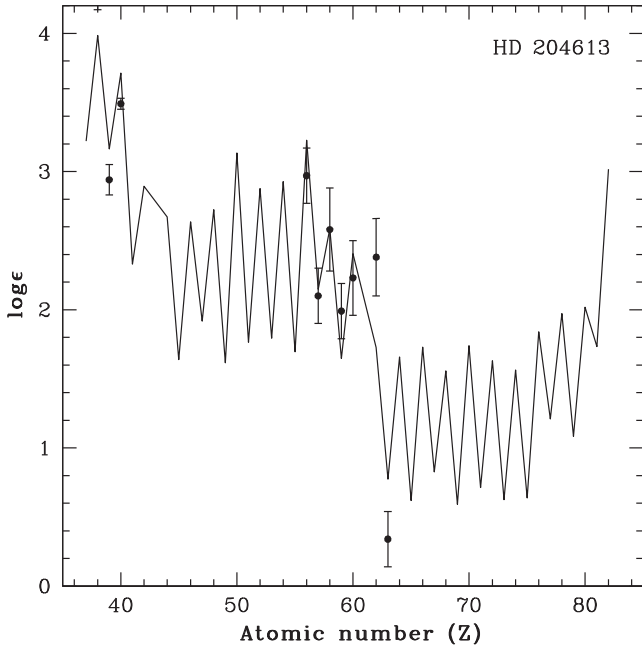


Figure 13. Solid curve represent the best fit for the parametric model function $\log \epsilon = A_s N_{si} + A_r N_{ri}$, where N_{si} and N_{ri} represent the abundances due to s- and r-process, respectively (Arlandini et al. 1999, Stellar model, scaled to the metallicity of the star). The points with error bars indicate the observed abundances in HD 204613.

with a metallicity of -1.49 and $[C/Fe]$ ratio of 1.01 shows a mild enhancement in neutron-capture elements. Estimated $[Ba/Fe]$ for this object is ~ 0.57 .

In the sample, we have two confirmed binaries; HD 122202 and HD 204613 with periods 1290 ± 9 d and 878 ± 4 d, respectively (McClure 1997). The estimated $[C/Fe]$ is < 1 for all objects except for HD 55496. Thus, if we follow the CEMP stars classification of Beers & Christlieb (2005), only HD 55496 falls into the CEMP star group with $[Fe/H] \leq -1.0$ and $[C/Fe] \geq 1.0$. Several authors have adopted $[C/Fe] \geq 0.5$ to define CEMP stars (Ryan et al. 2005; Carollo et al. 2012). In our sample, four objects have $[C/Fe] \geq 0.5$. The Objects HD 89668, HD 111721, HD 148897, HD 164922 and HD 167768 give near solar or mildly under solar value for $[C/Fe]$. These objects also show near-solar or underabundant $[Ba/Fe]$ value. Although other heavy elements are mildly enhanced in these objects, these objects are unlikely to belong to the group of CEMP or classical CH stars.

We have estimated the Ba abundance for all the objects in our sample, however abundance of Eu could be measured only for four objects. Following the abundance criteria of Beers & Christlieb (2005) based on Ba and Eu abundances, two objects HD 104979 and HD 204613 with $[Ba/Eu] \geq 0.5$, fall into the group of CEMP-s stars. Both the objects show enhancement in heavy elements. In HD 104979, the heavy s-process elements are more enhanced than the light s-process elements with $[hs/l_s] \sim 0.18$. In HD 204613, the light s-process elements are more enhanced with $[hs/l_s] = -0.1$. The parametric-model-based analysis indicates higher contribution from the s-process than that of r-process to the abundances of heavy elements observed in these objects.

CH stars are low-mass objects. Eight objects in our sample for which we could estimate stellar masses are found to be low-mass objects with masses in the range $0.6\text{--}1.6 M_{\odot}$. Stellar masses could not be estimated for the rest four objects as the parallax estimates

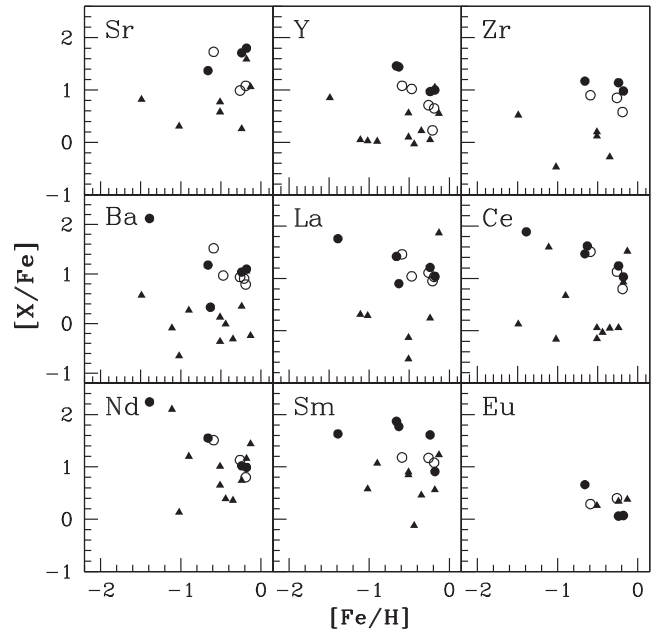


Figure 14. Abundance ratios of heavy elements observed in the programme stars with respect to $[Fe/H]$. The confirmed binaries are shown with solid circles, the objects with limited radial velocity information are shown with open circles, and the rest of the objects are indicated with solid triangles. The abundance ratios show a large scatter with respect to metallicity.

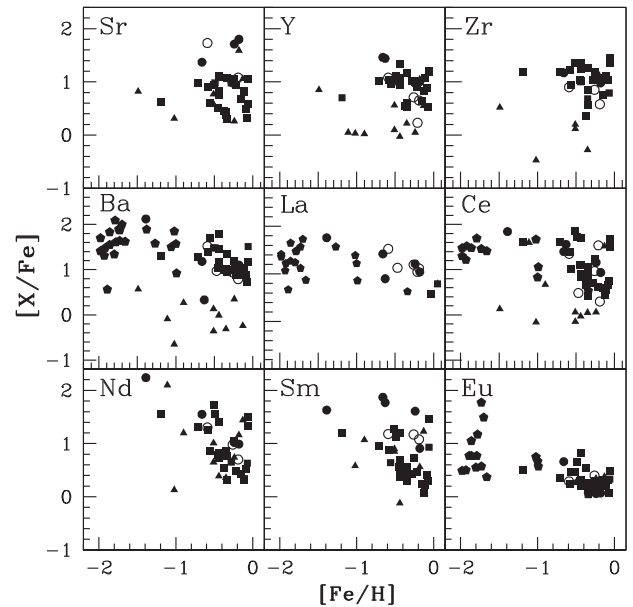


Figure 15. Estimated abundance ratios of Ba, La, Ce and Eu with respect to Fe are plotted in this figure where solid circles indicates the confirmed binaries, open circles indicate the objects with limited radial velocity information and the solid triangles indicate the rest of the objects in our sample. The abundance ratios are compared with the abundance ratios observed in CEMP stars (solid pentagons) from Masseron et al. (2010) and Ba stars (solid squares) from Allen & Barbuy (2006a).

are not available in the literature. These four objects HD 122202, HD 89968, HD 126681 and HD 164922 have $[Ba/Fe] < 0.33$ with HD 89968 giving a $[Ba/Fe]$ estimate of ~ -0.24 . These objects do not qualify as CH stars. Abundance ratios of the sample stars show a large scatter with respect to $[Fe/H]$ (Fig. 14). $[X/Fe]$ ratios

of the heavy elements for most of the objects belonging to group 3 are distinctly lower than their counterparts observed in the stars of group 1 and 2. Abundance ratios of Eu with respect to Fe observed in three stars of group 3 show similar values as those seen in two objects of group 2.

Population I Ba stars are believed to be metal-rich counterparts of CH stars. Both CH stars and Ba stars are known to show enhancement in heavy elements. A comparison of the abundance ratios of heavy elements with those observed in barium stars (solid squares) and CEMP stars from Masseron et al. (2010, solid pentagons) within the metallicity range 0.2 to -2.2 show that the group 3 objects distinctly return lower $[X/Fe]$ ($[Zr/Fe]$, $[Ba/Fe]$, $[La/Fe]$ and $[Ce/Fe]$; Fig. 15). These objects do not seem to belong to the group of CH stars as far as the chemical composition of heavy elements are concerned.

ACKNOWLEDGEMENTS

We thank the referee, for valuable comments which have improved our paper considerably. This work made use of the SIMBAD astronomical data base, operated at CDS, Strasbourg, France, and the NASA ADS, USA. Fundings from CSIR and DST project No. SB/S2/HEP-010/2013 are gratefully acknowledged.

REFERENCES

- Abia C., Rebolo R., Beckman J. E., Crivellari L., 1988, *A&A*, 206, 100
 Allen D. M., Barbay B., 2006a, *A&A*, 454, 895
 Allen D. M., Barbay B., 2006b, *A&A*, 454, 917
 Alonso A., Arribas S., Martinez-Roger C., 1996, *A&A*, 313, 873
 Alonso A., Arribas S., Martinez-Roger C., 1999, *A&AS*, 140, 261
 Aoki W. et al., 2001, *ApJ*, 561, 346
 Aoki W., Norris J. E., Ryan S. G., Beers T. C., Ando H., 2002a, *ApJ*, 567, 1166
 Aoki W., Ryan S. G., Norris J. E., Beers T. C., Hiroyasu A., Tsangarides S., 2002b, *ApJ*, 580, 1149
 Aoki W. et al., 2005, *ApJ*, 632, 611
 Aoki W., Beers T. C., Christlieb N., Norris J. E., Ryan S. G., Tsangarides S., 2007, *ApJ*, 655, 492
 Arlandini C., Käppeler F., Wisshak K., Gallino R., Lugaro M., Busso M., Straniero O., 1999, *ApJ*, 525, 886
 Asplund M., Grevesse N., Sauval A. J., 2005, in Thomas G. B., III Frank N. B., eds, *ASP Conf. Ser. Vol. 336, Cosmic Abundances as Records of Stellar Evolution and Nucleosynthesis in Honor of David L. Lambert*. Astron. Soc. Pac., San Francisco, p. 25
 Baranne A. et al., 1996, *A&AS*, 119, 373
 Barbay B., Spite M., Spite F., Hill V., Cayrel R., Plez B., Petitjean P., 2005, *A&A*, 429, 1031
 Bartkevicius A., 1996, *Balt. Astron.*, 5, 217
 Beers T. C., Christlieb N., 2005, *ARA&A*, 43, 531
 Bidelman W. P., 1981, *AJ*, 86, 553
 Bond H. E., 1974, *ApJ*, 194, 95
 Busso M., Gallino R., Lambert D. L., Travaglio C., Smith V. V., 2001, *ApJ*, 557, 802
 Carollo D. et al., 2012, *ApJ*, 744, 195
 Cavallo R. M., Pilachowski C. A., Rebolo R., 1997, *PASP*, 109, 226
 Christlieb N., Green P. J., Wisotzki L., Reimers D., 2001, *A&A*, 375, 366
 Frasca A., Covino E., Spezzi L., Alcalá J. M., Marilli E., Fursez G., Gandolfi D., 2009, *A&A*, 508, 1313
 Fulbright J. P., 2000, *AJ*, 120, 1841
 Girardi L., Bressan A., Bertelli G., Chiosi C., 2000, *A&AS*, 141, 371
 Gontcharov G. A., 2006, *Astron. Lett.*, 32, 759
 Goswami A., 2005, *MNRAS*, 359, 531
 Goswami A., Karinkuzhi D., 2013, *A&A*, 549, 68
 Goswami A., Prantzos N., 2000, *A&A*, 359, 191
 Goswami A., Aoki W., 2010, *MNRAS*, 404, 253
 Goswami A., Wako A., Beers T. C., Christlieb N., Norris J., Ryan S. G., Tsangarides S., 2006, *MNRAS*, 372, 343
 Goswami A., Bama P., Shantikumar N. S., Devassy D., 2007, *Bull. Astron. Soc. India*, 35, 339
 Goswami A., Karinkuzhi D., Shantikumar N. S., 2010a, *MNRAS*, 402, 1111
 Goswami A., Subramania Athiray P., Karinkuzhi D., 2010b, in Chaudhuri R. K., Mekkaden M. V., Raveendran A. V., Satya Narayanan A., eds, *Recent Advances in Spectroscopy Theoretical, Astrophysical and Experimental Perspectives*. Springer-Verlag, Berlin, p. 211
 Gratton R. G., Sneden C., 1991, *A&A*, 241, 501
 Gratton R. G., Sneden C., 1994, *A&A*, 287, 927
 Gratton R. G., Carretta E., Castelli F., 1996, *A&A*, 314, 191
 Gratton R. G., Sneden C., Carretta E., Bragaglia A., 2000, *A&A*, 354, 169
 Jonsell K., Barklem P. S., Gustafsson B., Christlieb N., Hill V., Beers T. C., Holmberg J., 2006, *A&A*, 451, 651
 Karinkuzhi D., Goswami A., 2014, *MNRAS*, 440, 1095 (Paper I)
 Koleva M., Vazdekis A., 2012, *A&A*, 538, 143
 Kurucz R. L., 1995a, in Adelman S. J., Wiese W. L., eds, *ASP Conf. Ser. Vol. 78, Astrophysical Applications of Powerful New Databases*. Astron. Soc. Pac., San Francisco, p. 205
 Kurucz R. L., 1995b, in Sauval A. J., Blomme R., Grevesse N., eds, *ASP Conf. Ser. Vol. 81, Laboratory and Astronomical High Resolution Spectra*. Astron. Soc. Pac., San Francisco, p. 583
 Kyrolainen J., Tuominen I., Vilhu O., Virtanen H., 1986, *A&AS*, 65, 11
 Lambert D. L., Ries L. M., 1981, *ApJ*, 248, 228
 Lawler J. E., BonVallet G., Sneden C., 2001, *ApJ*, 556, 452
 Lü P. K., 1991, *AJ*, 101, 2229
 Lucatello S., Gratton R. G., Beers T. C., Carretta E., 2005, *ApJ*, 625, L833
 Luck R. E., 1991, *ApJS*, 75, 579
 Luck R. E., Bond H. E., 1991, *ApJS*, 77, 515
 Luck R. E., Heiter U., 2007, *AJ*, 133, 2464
 McClure R. D., 1983, *ApJ*, 268, 264
 McClure R. D., 1984, *ApJ*, 280, L31
 McClure R. D., 1997, *PASP*, 109, 536
 McClure R. D., Woodsworth W., 1990, *ApJ*, 352, 709
 MacConnell D. J., Frye R. L., Uggren A. R., 1972, *AJ*, 77, 384
 McWilliam A., 1990, *ApJS*, 74, 1075
 McWilliam A., 1998, *AJ*, 115, 1640
 Massarotti A., Latham D. W., Stefanik R. P., Fogel J., 2008, *AJ*, 135, 209
 Masseron T., Johnson J. A., Plez B., Van Eck S., Primas F., Goriely S., Jorissen A., 2010, *A&A*, 509, A93
 Mishenina T. V., Pignatari M., Korotin S. A., Soubiran C., Charbonnel C., Thielemann F.-K., Gorbaneva T. I., Basak N. Yu., 2013, *A&A*, 552, 128
 Moultaq J., Ilovaisky S. A., Prugniel P., Soubiran C., 2004, *PASP*, 116, 693
 Nidever D. L., Marcy G. W., Butler R. P., Fischer D. A., Vogt S. S., 2002, *ApJS*, 141, 503
 Nissen P. E., Schuster W. J., 2011, *A&A*, 530, 15
 Nissen P. E., Chen Y. Q., Schuster W. J., Zhao G., 2000, *A&A*, 353, 722
 Norris J. E., Ryan S. G., Beers T. C., 1997a, *ApJ*, 488, 350
 Norris J. E., Ryan S. G., Beers T. C., 1997b, *ApJ*, 489, L169
 Norris J. E., Ryan S. G., Beers T. C., Aoki W., Ando H., 2002, *ApJ*, 569, L107
 North P., Duquennoy A., 1991, *A&A*, 244, 335
 North P., Duquennoy A., 1992, in Duquennoy A., Meyer D., eds, *Binaries as Tracers of Stellar Formation*. Cambridge Univ. Press, Cambridge, p. 205
 North P., Berthet S., Lanz T., 1994, *A&A*, 281, 775
 Pilachowski C. A., Sneden C., Booth J., 1993, *ApJ*, 407, 699
 Pourbaix D. et al., 2004, *A&A*, 424, 727
 Prochaska J. X., McWilliam A., 2000, *ApJ*, 537, L57
 Prugniel P., Vauglin I., Koleva M., 2011, *A&A*, 531, 165
 Ramirez I., Melendez J., 2004, *ApJ*, 609, 417
 Rebolo R., Molero P., Beckman J. E., 1988, *A&A*, 192, 192
 Ryan S. G., Lambert D. L., 1995, *AJ*, 109, 2068
 Ryan S. G., Aoki W., Norris J. E., Beers T. C., 2005, *ApJ*, 635, 349
 Santos N. C. et al., 2011, *A&A*, 526, 112
 Siebert A. et al., 2011, *AJ*, 141, 187

- Smith V. V., 1984, *A&A*, 132, 326
 Smith V. V., Lambert D. L., 1986, *ApJ*, 303, 226
 Smith V. V., Coleman H., Lambert D. L., 1993, *ApJ*, 417, 287
 Sneden C., 1973, PhD thesis, Univ. Texas
 Sneden C., Lambert D. L., Pilachowski C. A., 1981, *ApJ*, 247, 1052
 Sneden C., McWilliam A., Preston G. W., Cowan J. J., Burris D. L., Armosky B. J., 1996, *ApJ*, 467, 819
 Soubiran C., Bienayme O., Mishenina T. V., Kovtyukh V. V., 2008, *A&A*, 480, 91
 Sousa S. G., Santos N. C., Israelian G., Mayor M., Udry S., 2011, *A&A*, 533, 141
 Sozzetti A., Torres G., Latham D. W., Stefanik R. P., Korzennik S. G., Boss A. P., Carney B. W., Laird J. B., 2009, *ApJ*, 697, 544
 Tomkin J., Lambert D. L., 1986, *ApJ*, 311, 819
 Tomkin J., Lemke M., Lambert D. L., Sneden C., 1992, *AJ*, 104, 1568
 Worley C. C., Hill V. J., Sobeck J., Carretta E., 2013, *A&A*, 553, A47

SUPPORTING INFORMATION

Additional Supporting Information may be found in the online version of this article:

Table 4A. Fe lines used for deriving atmospheric parameters.

Table 4B. Fe lines used for deriving atmospheric parameters.

Table 8A. Equivalent widths in mÅ of lines used for the calculation of light element abundances.

Table 8B. Equivalent widths in mÅ of lines used for the calculation of light element abundances.

Table 9A. Equivalent widths in mÅ of lines used for abundance determination of heavy elements.

Table 9B. Equivalent widths in mÅ of lines used for abundance determination of heavy elements.

(<http://mnras.oxfordjournals.org/lookup/suppl/doi:10.1093/mnras/stu2079/-/DC1>).

Please note: Oxford University Press are not responsible for the content or functionality of any supporting materials supplied by the authors. Any queries (other than missing material) should be directed to the corresponding author for the paper.

This paper has been typeset from a $\text{T}_{\text{E}}\text{X}/\text{L}^{\text{A}}\text{T}_{\text{E}}\text{X}$ file prepared by the author.